Global J. Environ. Sci. Manage. 9(4): 673-690, Autumn 2023, Serial #36

Global Journal of Environmental Science and Management
(GJESM)

Homepage: https://www.gjesm.net/

Podcasts

ORIGINAL RESEARCH PAPER

Coagulants for water based on activated aluminum alloys

R.G. Sarmurzina[1], G.I. Boiko[1], B.K. Kenzhaliyev[1], U.S. Karabalin[2], N.P.Lyubchenko[1], P.V. Kenyaikin[1,*], Zh.B. Ilmaliyev[1]

[1] *Satbayev University, Institute of Metallurgy and Ore Beneficiation JSC, Almaty, Kazakhstan*

[2] *Kazenergy Association, Astana, Kazakhstan*

ARTICLE INFO

Article History:
Received 23 October 2022
Revised 28 January 2022
Accepted 11 March 2023

Keywords:
Activated aluminum alloy
Aluminum polyoxychloride
Coagulant
Microstructure
Water treatment

ABSTRACT

BACKGROUND AND OBJECTIVES: The reduction of fresh water deficit and water-related morbidity is the most important problem of the state's national security. The effective treatment of natural water in industrialized areas from natural and anthropogenic pollutants is the main ecological task. Coagulation is one of the effective methods used to treat water chemically to purify it. Aluminum polyoxychlorides have gained popularity because of their advantages over coagulants—aluminum and iron sulfates. No production of aluminum polyoxychloride occurs in Kazakhstan despite the need for coagulants (the minimum need is assessed at about 11 thousand tons). The work is aimed at theoretical justification and experimental proof of a principally new approach to the development of aluminum polyoxychloride production technology based on activated aluminum alloys containing metal activators, such as gallium, indium, and tin from 0.5 to 5 percent weight. In addition, the goal is solving environmental issues associated with improving the drinking water quality and related to environmental pollution with wastewater.
METHODS: The microstructures, phase components, and elemental compositions of alloys and reaction products were studied by scanning electron microscopy/energy dispersive X-ray spectroscopy. The thermal effects of alloys were investigated usin thermogravimetry methods. Oil content in wastewater was determined by spectrophotometry. Oil particle dimensions and wastewater zero potentials were determined using electrophoretic light scattering method and residual turbidity by turbidimetry. Water quality assessment was included in the purified water analysis and comparison with the sanitary and epidemiological standards established for drinking water supply and wastewater intended for water discharge.
FINDINGS: The structures and compositions of activated aluminum alloy containing metal activators - gallium, indium, and tin - from 0.5 to 5 weight percent and aluminum polyoxychlorides based on it were studied using modern instrumental methods. The efficiency of the treatment of natural and oil-contaminated wastewater with aluminum polyoxychloride was assessed. The treated water parameters were within the norms established for drinking water supply and wastewater disposal by Sanitary Rules and Norms 2.1.4.559-96. The efficiency of potable water treatment reached 90–99 percent.
CONCLUSION: An effective and technologically simple method is developed for producing aluminum polyoxychloride. It involves dissolving an activated alloy in 1–5 percent hydrochloric acid, with an aluminum content of 98.5–85 percent. Alloy processing is carried out at temperatures ranging from 60 to 65 degree celsius. The temperature rises from 20 to 25 degree celsius to the specified optimum without heat supply from the outside due to the interaction among reagents. The process is completed in 2–3 hours. The results confirm that aluminum polyoxychloride is an effective coagulant for drinking and wastewater treatment. The treated water is within the established limits in terms of hydrogen potential, chemical oxygen demand, and turbidity. The water treatment method can be easily implemented.

DOI: 10.22035/gjesm.2023.04.02

NUMBER OF REFERENCES	NUMBER OF FIGURES	NUMBER OF TABLES
39	10	10

*Corresponding Author:
Email: *kenyaikin.p@gmail.com*
Phone: +7727 292 5787
ORCID: 0000-0002-4360-1573

Note: Discussion period for this manuscript open until January 1, 2024 on GJESM website at the "Show Article".

INTRODUCTION

Traditional coagulants based on iron and aluminum salts (Chen *et al*., 2018; Jiao *et al*., 2015), including titanium salts (Wang *et al.,* 2018; Xiao *et al.*, 2008; Zhao *et al.,* 2011), are widely used in the treatment of natural water (H_2O) and wastewater in the coagulation process to remove suspended solids and reduce turbidity and dissolved substances. In the conditions of water resource scarcity, severe environmental pollution, and tightening standard for the discharge of oil-contaminated wastewater into water bodies (Lee *et al*., 2017), research on the development of methods for obtaining effective coagulants and purification process and natural and wastewater disposal is significant and relevant. Polyaluminum chloride (PAC) is one of the widespread coagulants for water and wastewater treatment. The methods of producing aluminum polyoxychloride using metallic aluminum in the form of ingots, secondary raw materials (scrap), aluminum hydroxides, aluminum chloride, and aluminum oxide are discussed in detail in the works of He *et al*. (2019); Li *et al*. (2010); Zhang *et al*. (2017). Hydrochloric acid (HCl), aluminum chloride, aluminum sulfate, and low-basic aluminum chloride are used as chlorine (Cl)-containing reagents (Sychev *et al*., 2015), which have a low corrosivity (hydrogen potential pH = 1.0–2.5), allowing the use of equipment made of ordinary or low alloy steel. The methods of obtaining PAC using metallic aluminum are limited by the high costs of aluminum, corrosive environment, and process duration and application of a complex technological scheme with the circulation of the reaction mixture through a system of two reactors (Tokareva *et al*., 2020). Solving the issue of equipment and pipeline protection from corrosion is necessary when sufficiently concentrated HCl above 10 percent (%) is used and a reaction temperature is 95 degree celsius (°C). Special materials are used for equipment, including graphite reflux condensers, graphite grids in the reactor, and special steels. The method of obtaining PAC by the interaction of aluminum powder with an aluminum chloride solution is no less dangerous. A risk of explosion is possible due to the high activity of a specific surface area and increased reactivity. The application of aluminum oxides and hydroxides for the production of PAC is limited by the hard conditions of the process, the need to use freshly prepared aluminum hydroxide, multistage, the use of apparatus made of special materials, because the process takes place in an aggressive environment at high pressure and temperature (Masakbaeva *et al*., 2021). The cost of PAC obtained using these methods is quite high in the world market. Studing applying activated aluminum alloys (AAAs), which contain activating metals gallium (Ga), indium (In), tin (Sn) as reagents for aluminum polyoxychloride production, have not been found from the world state of art. Three, four, and multicomponent AAAs are used as sources for hydrogen storage (Sarmurzina *et al*., 2022a; Trowell *et al*., 2020); hydrogen production from water (He *et al*., 2017a, 2017b; Kumar *et al*., 2020; Pini *et al*., 2020; Qiao *et al*., 2019; Wei *et al*., 2018;); and alternative, renewable, and clean fuel sources (Xiao *et al*., 2019). Aluminum is alloyed with Ga, In, Sn, zinc (Zn), bismuth (Bi), cadmium (Cd), copper (Cu) metals for activation (Du *et al*., 2018; He *et al.,* 2020b; Wang *et al.,* 2012; Yang *et al*., 2017). The scientific novelty of this work lies in using AAAs to obtain a coagulant PAC for physical and chemical water purification from natural and anthropogenic pollutants, in improving water quality, in rejecting foreign products, in solving the problem of clean fresh water shortage, in increasing water supply sustainability to populations and industries, in improving national water security and sustainable state development, in developing efficient technological processes, in new technical solutions for the creation of AAAs with low prices, excluding the use of expensive components. The advantage of the obtained PAC with a high content of alumina (> 10%) and high basicity is that its use makes it possible to obtain high-quality drinking water with a low content of residual aluminum (0.05–0.10 milligram per liter (mg/L), which is more than two times less than the norm of the World Health Organization (0.20 mg /L). In addition, PAC is used in natural water purification at temperatures ranging from 4 °C to 8 °C, at doses 20%–25% lower than for aluminum sulfate. The pH of the treated water practically does not change. PAC has a high polymerization ability (Tang *et al*., 2015), which is accelerate flocculation and coagulated suspension settling, ensures the highest efficiency of water purification from suspended solids and metals, and reduces water corrosiveness (absence of excess sulfates), which has bactericidal properties. The mechanism of coagulation water treatment with aluminum polyoxychloride has been considered in existing works (Shamaei *et al*., 2018; Sun *et al*., 2019). According to Jiao, R *et al*. (2015), a distinctive feature

of aluminum polyoxychloride is that aluminum exists in the form of aquahydroxo complexes. These complexes have high charges, molecular weights, and specific surface areas, which allow the products of their hydrolysis to capture, adsorb, and thereby remove suspended colloidal impurities from the treated water. The current study aims for the theoretical substantiation and experimental proof of a fundamentally new approach to the development of technology for the production of aluminum polyoxychloride based on AAAs containing activating metals: Ga, In, and Sn from 0.5 weight percent (wt%) to 5 wt%. It also involves the investigation of the microstructures, compositions, and thermal properties of AAAs with metal activators: Ga, In, Sn in amounts ranging from 0.5 wt% to 5 wt%; development of a method for producing aluminum polyoxychloride based on AAAs used as coagulants in drinking water purification; evaluation of the efficiency of natural and oil-contaminated wastewater purification with aluminum polyoxychloride. This study is carried out at Satbayev University, Joint-stock company (JSC) Institute of Metallurgy and Enrichment, Republic of Kazakhstan during the 2022–2023 period.

MATERIALS AND METHODS

Aluminium (purity 99.85%) in granules was purchased from Aluminium Smelter JSC, the only aluminium producer in Kazakhstan, part of the Eurasian Group. Ga (purity 99.99%), in the form of cylindrical ingots with weights ranging from 900 grams (g) to 1000 g, was purchased from Kazakhstan Aluminium Smelter JSC; its melting point was 156.59 °C and density was 7.362 (+20 °C, grams per cubic centimeter (g/cm^3). In (purity 99.999%) in the form of cylindrical ingots with weights ranging from 0.05 g to 1000 g was purchased from Aluminium Smelter JSC; its melting point was 29.80 °C and density was 5.904 (+20 °C, g/cm^3). Sn was in ingots with weights from 22 kilogram (kg) to 26 kg; Sn content was 99.565%, and its melting point was 231.91 °C. HCI (chemical purity) with azeotropic mixture boiling point (20.22% by mass) –108.6 °C, density 1.16 g/cm^3 (35%), was used without additional purification.

*Sodium hydroxide (*chemical purity) *was used without additional purification.*

AAAs - Rau-98.5, Rau-97, and Rau-85 - containing activator metals, such as Ga, In, and Sn (from 0.5 wt% to 5 wt%), were obtained by melting (Sarmurzina *et al*., 2022a; 2022b). Aluminum was melted in an inert gas atmosphere in an alundumina crucible in a muffle furnace at 850 °C. Activating additives stirred to achieve melt homogeneity were put in the molten aluminum. The heating–holding–cooling cycle lasted 1 hour, then the melt was poured into fabricated steel molds with an outer diameter of 60 millimeters (mm), inner of 40 mm, and a height of 40–80 mm. Powder with given particle sizes of 80–1250 micrometers (μm) was made from ingots by changing gaps among crusher jaws (mm): 1, 2, 5 and 10. Aluminum alloys were characterized using a scanning electron microscope with energy dispersive X-rays (SEM/EDX). The X-ray spectral analysis of alloys was performed with an X-ray fluorescence spectrometer—X-Ray Innov-X systems (United States of America). The phase compositions of alloys were analyzed using X-ray diffraction method (XRD) on a D8 ADVANCE diffractometer (Bruker, Germany), at α- Cu tube voltage 40 kilovolt (kV) and current 40 milliamp (mA). The elemental composition analysis for the samples and photographing in various radiation kinds were performed using energy dispersive spectrometer—INCA Energy by Oxford Instruments (United Kingdom) mounted on electron-probe microanalyzer Superprobe 733 by JEOL Limited trade development (Ltd) (Japan), at accelerating voltage 25 kV and probe current 25 nanoamp (nA). The thermal analysis of alloys was performed using a synchronous thermal analysis device—simultaneous thermal analyzer (STA) 449 F3 Jupiter (Germany). The furnace space was evacuated before heating (vacuum level reached ~92%) and then purged with inert gas for 5 minutes (min). Heating was performed at a rate of 10 degrees Celsius per minute (°C/min) in an atmosphere of highly purified argon. The total volume of incoming gas was kept within 110 milliliters per minute (mL/min). The results obtained with the STA 449 F3 Jupiter were processed using NETZSCH Proteus software. X-ray powder images were recorded on a D8 Advance diffractometer (Bruker), at α-Cu tube voltage 40 kV and current 40 mA. The processing of obtained data from diffractograms and calculation of interplanar distances was performed using the EVA software. Sample interpretation and phase search were conducted using the search/match program using the powder diffractometer database (PDF)-2. Aluminum polyoxychloride, with the mass fraction of AI on aluminium oxide (Al_2O_3) 33.2%–36.9% and basicity

56%–67%, corresponding to GuoBiao (GB) 15892-2009, was obtained according to the developed method used to treat aluminum-containing alloys by 1%–5% HCI solution at a ratio of 1:50. The dissolution process for aluminum-containing alloys proceeds with sufficient speed, accompanied by a uniform release of hydrogen and increasing temperature of the reaction medium. The temperature rose from room temperature to the optimum temperature (50 °C–90 °C), without heat input from outside, due to the interaction among reagents. The process was completed in 2–3 hours. The high reactivity of aluminum-containing alloys was due to the presence of activating metals (Ga, In, and Sn) contributing to the mechanical loosening of surfaces, heterogeneity of alloys, and formation of micro-galvanic elements. Activating metals form easily fusible eutectics with aluminum in the region of immiscibility in the liquid phase, resulting in the destruction of a dense layer of aluminum oxide and a sharp increase in its chemical activity. The amount of hydrogen released during the interaction of aluminum alloys with HCI was measured on a drum gas meter. All experiments were repeated at least three times and were performed at 25 °C and a humidity of 60%. The water heating temperature was measured with a thermometer with an accuracy of 0.1 °C. The hydrogen release rate was calculated using Eq. 1 in milliliters per gram per minute (mL/g/min) (Sarmurzina *et al*., 2018).

$$W_{\mathrm{H}} = \frac{V}{m\Delta t} \quad (1)$$

Where, *V* is the amount of hydrogen released; *m* is the mass of the alloy sample; Dt is time between two measurements of gas clock readings.

The theoretical amount of hydrogen was calculated based on the generation of 1.244 L of hydrogen per 1 g Al under standard conditions (273 Kelvin (K), 1 atm). Sampling; determining initial water quality parameters; and process controlling aluminum, turbidity, hydrogen potential, and chemical oxygen consumption were performed according to standard procedures. Oil content in wastewater was determined with spectrophotometer SPEKOL 1300 (Analytik Jena). Studies on oil particle size and wastewater zeta potential before and after a coagulant treatment were executed using the Malvern Zetasizer NanoZS 90 particle size analyzer. The water treatment with the obtained coagulants was performed as follows: 200 mL of test natural water was poured into a 250 mL beaker, and a given amount of coagulant solution was introduced into it under constant quick stirring (180 revolutions per minute (rpm). The sample was stirred for 1 min with a continuous pH control. Subsequently, the stirrer was switched to slow stirring −50 rpm for 10 min. The residual turbidity was measured directly using a HACH 2100Q Turbidimeter.

RESULTS AND DISCUSSION

The X-ray spectral analysis of Rau-85 aluminum alloy obtained using the X-Ray Innov-X system spectrometer showed that the main component of the activated Rau-85 alloy was aluminum with the content of 85.71%. The metal content in the alloy insignificantly differed from the initial ratio of metals taken for the alloy preparation. The Rau-85 alloy contained trace amounts of impurities of metals not used as initial components: iron (Fe), Cd, lead (Pb), and Bi in amounts from 0.01% to 0.02%, and Fe content reached 0.09. SEM images and EDXs maps of the Rau-85 alloy sample surface are shown in Fig. 1. The study allowed us to obtain a general picture of the alloy surface, fractogram of the fracture surface, distribution of dissolved elements in the alloy, and their contents in some local areas of the sample by microprobe with a diameter of 1 μm (Fig. 1). The lighter areas in the micrograph indicate the presence of liquid eutectics of metal activators on aluminum grains (He *et al*., 2020a; Sarmurzina *et al*., 2022a; 2022b). The EDXs analysis results for the samples of bright white grains and aluminum alloy matrcies are illustrated in Fig. 1 and Table 1. Based on the data presented, concluding that the bright white grains are heterogeneous in composition is possible. The

Table 1: Results of energy dispersive X-ray spectroscopy of the Rau-85 alloy (Sarmurzina *et al*., 2022a)

		Element content, weight (%)				
Spectra	Grain	Al	Ga	In	Sn	Total
Spectrum 1	Bright white grain	3.04	5.90	69.37	21.70	100.00
Spectrum 2	Bright white grain	2.26	3.59	72.42	21.70	100.00
Spectrum 3	Matrix gray in the photo	58.49	12.54	17.70	11.27	100.00

activating components—Ga, In, Sn—in the alloy participate in the formation of complex eutectics and have a different distribution in the amount and on the surface of aluminum.

The thermogravimetric analysis method was used to obtain information on the melting temperatures of AAAs. The thermograms (TGs) of activated Rau-85 alloy are shown in Figs. 2 and 3.

The differential thermal analysis (DTA) curve recorded an exothermic effect with a peak at 556 °C and an endothermic effect with an extremum at 639 °C. The dDTA curve recorded endothermic effects with extremums at 113.9 °C and 568.5 °C. The process of surface oxidation of pellets caused the exothermic effect. The endothermic effect with an extremum at 639 °C on the DTA curve could be a manifestation of monotectic reaction in the In–Al system (Lyakishev, 1996). The endothermic effect with an extremum at 113.9 °C on the DTA curve could be a manifestation of melting in the Al–Ga system compound with Ga content ~84%–86%. Alternatively, the effect could be a manifestation of melting in the Ga–In system compound with In content ~80%. The endothermic effect with the extremum at 568.5 °C on the dDTA curve could be a manifestation of the melting in the Al–Ga system compound with Ga content ~20%. Three exothermic effects were recorded on the curves obtained during cooling at a rate of 13 °C/min. The first peak on the DTA curve was 599.7 °C. It reflected solid phase precipitation from the melt and one more liquid (monotectic reaction) in the In–Al system. The second peak at 619.4 °C appeared on the DTA curve. It showed aluminum crystallization. The third peak −571.8 °C reflected the crystallization of Al–Ga alloy

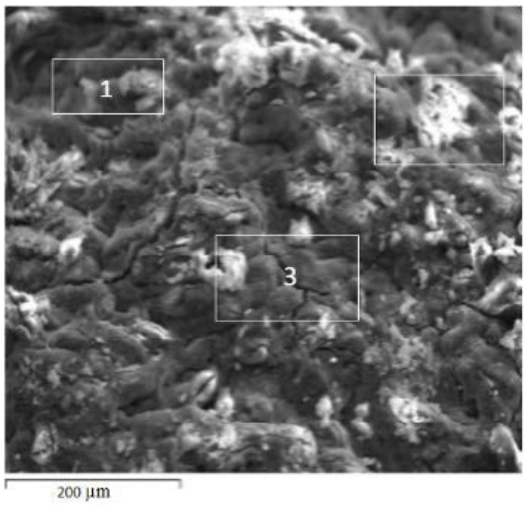

Fig. 1: SEM image of the activated Rau-85 alloy surface in secondary electrons (Sarmurzina *et al*., 2022a)

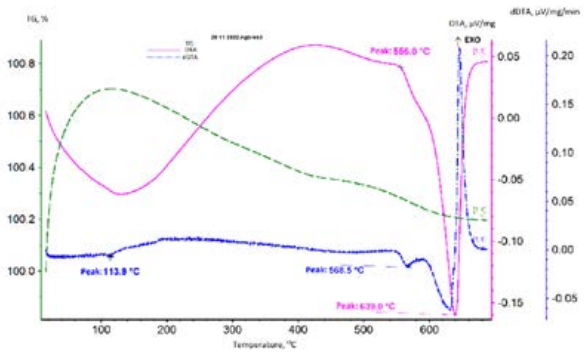

Fig. 2: Thermal analysis of activated Rau-85 alloy

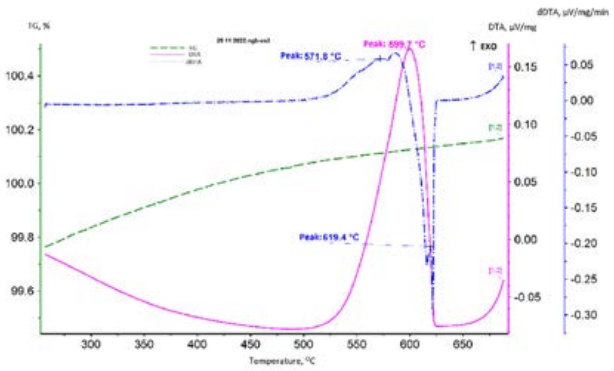

Fig. 3: Thermal analysis of activated Rau-85 alloy (cooling)

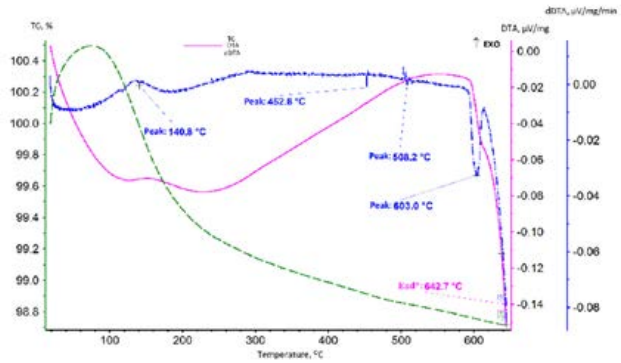

Fig. 4: Thermal analysis of activated Rau-97 alloy

with ~10%–12% Ga content.

The TGs of activated Rau-97 alloy with the content of In, Ga, and Sn 1:1:1 are shown in Figs. 4 and 5. Individual alloy pellets were selected to prevent intense surface oxidation for the thermal analysis of the activated Rau-97 alloy. The samples were heated to 643 °C. Endothermic effects with extremums at 140.8 °C, 452.8 °C, 508.2 °C, and 603 °C were recorded on the DTA curve. The first effect (140.8 °C) could be presumably attributed to the manifestation of the compound from the In–Sn system. A peritectic reaction In and liquid →ß were observed at this temperature, where ß was an intermediate phase with a face-centered cubic structure (according to other data, it may be body-centered cubic structure structure). Other effects probably belonged to compounds from the Al–Ga system. Thus, a liquid phase was formed in the Al–Ga alloy at 452.8 °C, with ~40% Ga content, and a liquid phase was formed in the Al–Ga alloy at 508.2 °C, with ~30% Ga content. The endothermic effect with extremum at 603 °C showed the formation of the liquid phase in the Al–Ga alloy, with ~10% Ga content, that is, the alloy contains Ga with different qualitative and quantitative compositions.

The curves obtained during cooling at a rate of 13 °C/min recorded two exothermic effects (Fig. 5). The first peak on the DTA curve was at 620.7 °C. It showed aluminum crystallization. The second peak at 586.6 °C appeared on the DTA curve. It showed crystallization of Al–Ga alloy with ~10% Ga.

Two endothermic effects were found on the DTA curve of Rau-98.5 alloy (Fig. 6a). The most intensive one had the maximum development at 663.6 °C. The extremum of the less intensive effect corresponded to 611 °C. The endothermic effect of 663.6 °C most likely showed aluminum melting. A bit elevated melting temperature could be caused by the presence of some impurities, specifically Al_2O_3. If the attention was paid to the dDTA curve in the

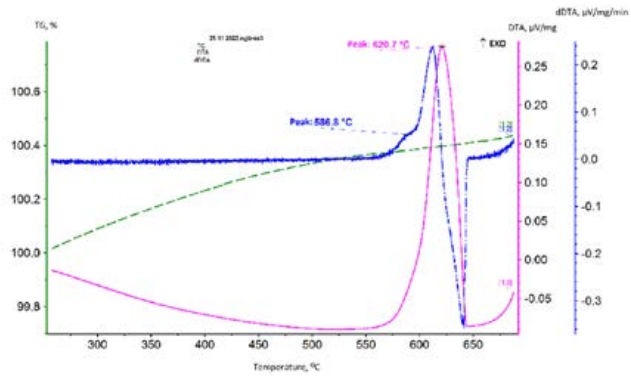

Fig. 5: Thermal analysis of activated Rau-97 alloy (cooling)

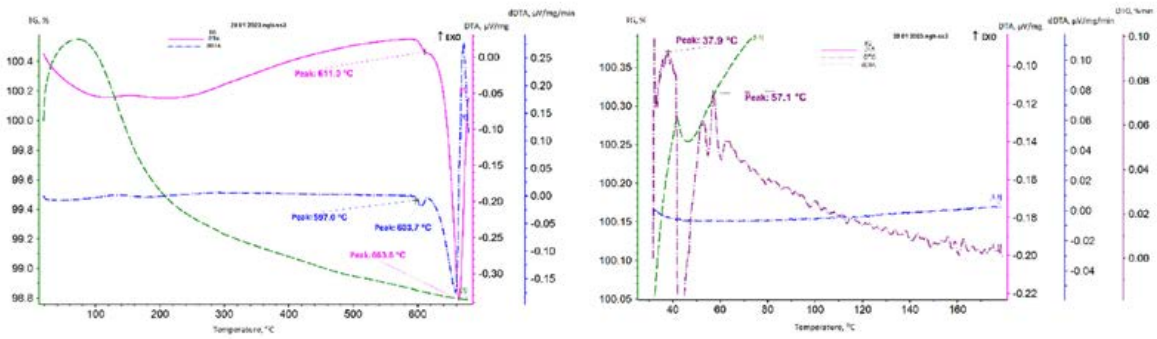

(a) (b)

Fig. 6: Thermal analysis of activated Rau-98,5 alloy (a) enlarged image of the dDTA curve within the considered temperature segment with extremum at 611 °C (b)

endothermic effect area with an extremum at 611 °C, then seeing that several effects appeared in the considered temperature interval was possible.

Fig. 6b shows an enlarged image of the dDTA curve in the temperature interval under consideration. Three endothermic effects with extremums at 597 °C, 603.7 °C, and 607 °C appeared. Presumably, this is a representation of the melting of Al–Ga system alloys with the content that is close in Ga-content value. No effects showing the presence of other phases were detected. Practically, the same effects were recorded. An exothermic effect with a peak at 596.1 °C, showing the surface oxidation in aluminum particles by residual oxygen, also appeared. An increase in the mass of the sample was recorded at the initial stage of heating. It could be seen from the thermogram (TG) curve course. The derivative thermogravimetric (DTG) curve showed maximums at 37.9 °C and 57.1 °C. We may assume that the oxidation of the In surface (37.9 °C) and the molten In surface (57.1 °C) takes place here. The presence of In was detected possibly indirectly. The X-ray diffraction analysis (XRD) of AAAs revealed that the alloys contained eutectic Ga with the composition ($Al_{0.95}$ $Ga_{0.05}$), binary intermetallic In with Sn $(In_3Sn)_{0.5}$; $(InSn_4)_{0.2}$; $In_{0.18}$ $Sn_{0.82}$, $In_{1.74}Sn_{0.26}$, $In_{0.2}Sn_{0.8}$. Their total percentage depended on the amount of activating additive in the alloy (Table 2).

The synthesis of PAC was performed by the interaction of AAAs with HCI. AAAs easily reacted with the aqueous solutions of HCI (1%–5%) at 20 °C–25 °C. The reaction was accompanied with heat and hydrogen emissions. Aluminum alloy was introduced into HCI solution in portions to prevent reaction

mass overheating. Multiple injections of activated aluminum created conditions for the directional hydrolysis of aluminum chloride and formation of polyoxychloride with the desired characteristics. Basic salt was formed during the hydrolysis of aluminum chloride. Hydrolysis is assumed to proceed by Al^{3+} cation (Novakov and Radchenko, 2013; Wei *et al.*, 2015; Zhang*et al.*, 2015). During hydrolysis, the Al^{3+} ion tears off the OH^- hydroxide ions from the water molecule, releasing H^+ cations. As hydrolysis deepens and the pH of the medium rises to neutral or weakly alkaline, the interaction among products results in the formation of polymeric hydroxocomplexes or colloidal aluminum hydroxide (Dayarathne *et al.*, 2021). The reaction is complicated by acid-base equilibrium with the position that depends on many factors: the pH value and temperature of the solution, the concentration and initial form of aluminum, and the activity of the anion present (Novakov and Radchenko, 2013). The structure of PAC depends on the pH of the medium. The product is prone to hydrolysis and has a strong effect on the pH of its aqueous solution, giving it an acidic reaction. The EDX analysis of the alloy reaction product with HCI showed that the CI content increases as the concentration of HCI solution in the product increases and is 34.34%. The CI content is 14.45% for the product based on Rau-85 and 13.34% for the product based on Rau-97 in the alloy reaction product with HCI of lower concentration. The observed dependence is the characteristic for Rau-85 and Rau-97-based PAC (Table 3).

A study of the reactions of AAAs with aqueous solutions of HCI revealed that the addition of AAAs to HCI solutions is accompanied by a heating of the reaction mixture from 50 °C to 90 °C. The temperature depends on the HCI concentration, the alloy-to-acid ratio, and the composition of the used alloy. In this research, the reaction was heterogeneous and ran on the solid–liquid interface. The amount of heat released and the speed of the chemical reaction largely depended on the contact surface area, including the chemical composition of the aluminum alloy. The period of rapid reaction lasted about 30–40 min, then its rate gradually slowed down. Curves of heat release and volume of released hydrogen during PAC synthesis, depending on the HCI concentration and multiplicity of AAA addition to the acid solution, are shown in Figs. 7 and 8.

The analysis allowed us to conclude that the amount of gas released and the rate of its release depended on the HCI concentration and the alloy composition during the process at 25 °C. When the HCI concentration increased from 1% to 5%, the hydrogen release rate increased. The reaction temperature, the amount of H_2 released, and the rate of its release increased as the acid concentration increased, reaching the theoretically calculated value. The reaction proceeded without an induction period and ended within 20–30 min. The conversion reached 95%–100%. The results showed that the treatment of aluminum-containing alloys activated by In 0.5 wt%–5 wt%, Ga 0.5 wt%–5 wt%, Sn 0.5 wt%–5 wt%, containing 98.5%, 97%, and 85% aluminum, respectively with 1%–5% aqueous HCI solutions,

Table 2: X-ray phase analysis of AAAs

Pattern number	Compound name	Formula	S-Q,%
	Rau-85		
PDF 00-004-0787	Aluminum, syn	Al	79.0
PDF 01-074-5208	Aluminum Gallium	$(Al_{0.95}Ga_{0.05})$	11.4
PDF 01-077-2745	Indium Tin	$(In_3Sn)_{0.5}$	5.3
PDF 01-085-4243	Indium Tin	$(InSn_4)_{0.2}$	4.3
	Rau-97		
PDF 00-004-0787	Aluminum, syn	Al	87.8
PDF 01-074-5208	Aluminum Gallium	$(Al_{0.95}Ga_{0.05})$	6.4
PDF 01-077-2745	Indium Tin	$(In_3Sn)_{0.5}$	3.9
PDF 01-073-9037	Indium Tin	$In_{0.18}Sn_{0.82}$	1.8
	Rau-98.5		
PDF 00-004-0787	Aluminum, syn	Al	25.0
PDF 01-074-5208	Aluminum Gallium	$(Al_{0.95}Ga_{0.05})$	67.0
PDF 01-077-2747	Indium Tin	$In_{1.74}Sn_{0.26}$	3.4
PDF 00-048-1547	Indium Tin	$In_{0.2}Sn_{0.8}$	2.3
PDF 01-077-3457	Tin	Sn	1.5
PDF 00-037-1462	Aluminum Oxide	Al_2O_3	0.8

Table 3: Results of X-ray elemental analysis of AAAs and their reaction products with HCI

Element, W (%)	Rau-85	Product		
		Rau-85 after treatment with 5% HCI solution,	Rau-85 after treatment with 1% HCI solution	Rau-97 after treatment with 1% HCI solution
Al	53.89	20.33	21.02	23.04
O	35.76	43.11	47.44	53.19
In	4.84	0.62	0.04	0.04
Ga	2.43	0.93	1.25	0.23
Sn	3.07	0.66	0.04	0.04
CI	-	34.34	14.45	13.34

Single addition of activated alloys to HCI solution, EDX analysis. Alloy: HCI ratio (1:50)

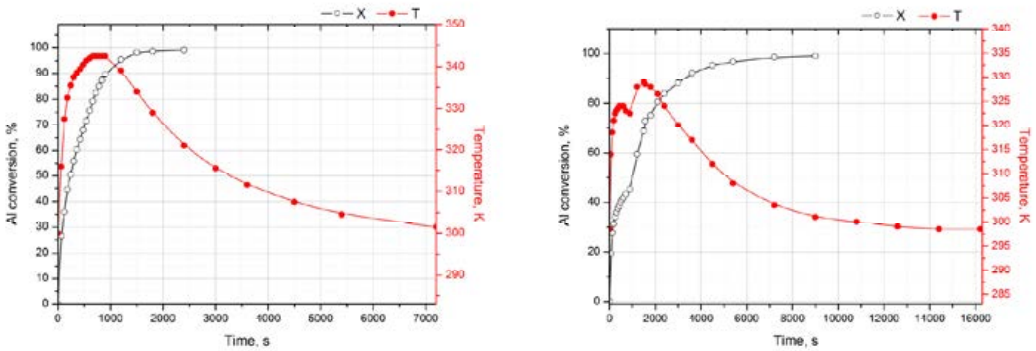

Fig. 7: Curves of process temperature and aluminum conversion vs. time, in the synthesis of coagulant based on Rau-97 and 3% HCl (1:50): a) single addition, b) double addition

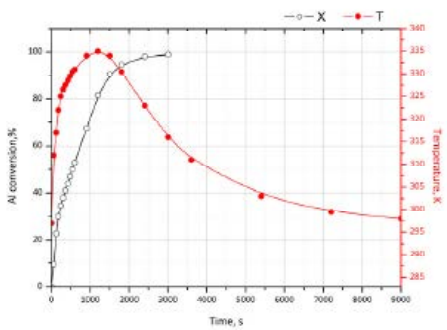

Fig. 8: Curves of process temperature and aluminum conversion vs. time for the synthesis of a coagulant based on Rau-98.5 (single addition) and 3% HCl (1:50)

resulted in sufficient heat emission to conduct the process without heating the solution and allowed to gain aluminum polyoxychloride with necessary basicity degree 41%–82.6% and with mass fraction Al_2O_3 30%–48% according to dissolution conditions. When the activating metals were dissolved in acid, they did not pass into the solution but roll into balls forming eutectic low-temperature alloys, settled at the bottom of the reactor unchanged, and could be reused for the preparation of aluminum-containing alloys. This property of a metal activator ensures the manufacturability of the process and its economic feasibility because the price of the alloy corresponds to the price of the original aluminum used. The basicity of a coagulant characterized the substitution degree of CI atom by hydroxyl group in aluminum chloride during the basic salt formation. Aluminum polyoxychloride solutions had pH ranging from 2.3 to

4.2, and the mass fraction of aluminum in terms of Al_2O_3 from 4.5% to 15.75%. A study of diffractograms of reaction product samples of activated Rau-85 alloy with 1% HCl solution (Coagulant No. 11, Al_20_3 content [31%], basicity [66.9%]) and of activated Rau-97 alloy with 1% HCl solution (Coagulant No. 15, Al_20_3 content [33.1%], basicity [62.7%]) resulted in the conclusion that the product was a mixture of crystal and amorphous phases. The XRD results indicated that the reaction products were heterogeneous in composition (Table 4). The compositions of the phases formed and their percentages depended on the nature of the alloys used for the reactions and reaction conditions (acid concentration, temperature).

Infrared (IR)-spectral analysis of interaction products of AAAs with HCl

The IR spectra of coagulants based on aluminum alloy Rau-85 (No. 11) and Rau-97 (No. 15) were recorded on the fourier-transform IR spectrometer "Avatar 370 CsI" in the spectral range 4000-300/cm from products in the form of tablets prepared by pressing, 2 mg sample and 200 mg potassium bromate (KBr), and in Vaseline oil-based suspension in thallium bromoiodide windows. A spectrum of Vaseline oil was taken as a reference spectrum. Attachment for the experiment: Transmission Enhanced Synchronous Protocol (Fig. 9).

An intense band of valent vibrations vOH – 3451/cm and a band of strain vibrations δ HOH – 1635/cm of water molecules were found in the spectra of Coagulants Nos. 11 and 15 (Nakamoto, 2009). Poly aluminum polynuclear hydroxo complex, aluminum hydroxide chloride hydrate $Al_{13}(OH)_{30}$ Cl $_9$ · 15 H_2O – 3451, 1635, 983, 726, 631, 553, 366/cm. The IR spectra of the products were similar and correspond to the compound—aluminum polyoxychloride. Based on the sources (Novakov and Radchenko, 2013; Tang *et al*., 2015) and data obtained in this work, when coagulants were introduced into water, their dissociation occurred. The polyvalent cations of the coagulant Al^{3+} formed in this case entered into ionic exchange with cations of the adsorption layer of negatively charged colloidal particles of pollution, reducing their stability (Wei *et al*., 2015). When working solutions of the PAC coagulant were prepared, the aluminum ion was assumed to exist in the form of an aqua complex $[Al(H_2O)_6]^3$ of octahedral structure in dilute aqueous solutions at pH ≤ 3 (Novakov and Radchenko, 2013). During the coagulation process, PAC hydrolysis resulted in the formation of polynuclear aquahydroxocomplexes of monomeric, polymeric, or amorphous aggregates due to the presence of a surface acid shell. It increased the intensification of wastewater treatment of suspended solids and metals. The high polymerization ability accelerated flake formation and precipitation. The hydrolysis reaction of aluminum polyoxychloride occured spontaneously in an aqueous solution (Grechanikov *et al*., 2010). The products were complexes of the general formula $Al[(OH)_3Al]n^{3+}$, complex $Al_6(OH)_{15}^{3+}$ $Al[(OH)_5Al_2]n^{3+}$, $Al_{13}(OH)_3^{7+}$; $Al(OH)_2^{4+}$, $Al_{2+n}(OH)_{3n}Cl_6$ (Grechanikov *et al*., 2010). When a certain hydrolysis degree was reached, the polymerization stage became preferable. According to Novakov and Radchenko

Table 4: Comparative results of semi-quantitative XRD of crystalline phases of reaction products based on Rau-85 alloy (Coagulant No. 11) and Rau-97 alloy (Coagulant No. 15)

Pattern number	Compound name	Formula	S-Q (%)	
			Coagulant No. 11	Coagulant No. 15
PDF 00-061-0795	Poly aluminum, aluminum polynuclear hydroxo complex, PAL | Aluminum Hydroxide Chloride Hydrate	$Al_{13}(OH)_{30}Cl_9 \cdot 15H_2O$	85.7	100.0
PDF 00-037-1377	δ-Al (O H)3 | Aluminum Hydroxide	$Al(OH)_3$	5.7	
PDF 01-088-1609	δ-Al Al1.67 O4 | Aluminum Oxide	$AlAl_{1.67}O_4$	4.8	
PDF 01-078-4581	δ-Al O (O H) | Aluminum Oxide Hydroxide	AlO (OH)	3.8	

Images were taken on a D8 Advance (Bruker), α-Cu tube voltage 40 kV, current 40 mA. The processing of the obtained data from diffractograms and the calculation of interplanar distances were performed using EVA software. Sample interpretation and phase search were performed by search/match using PDF-2.

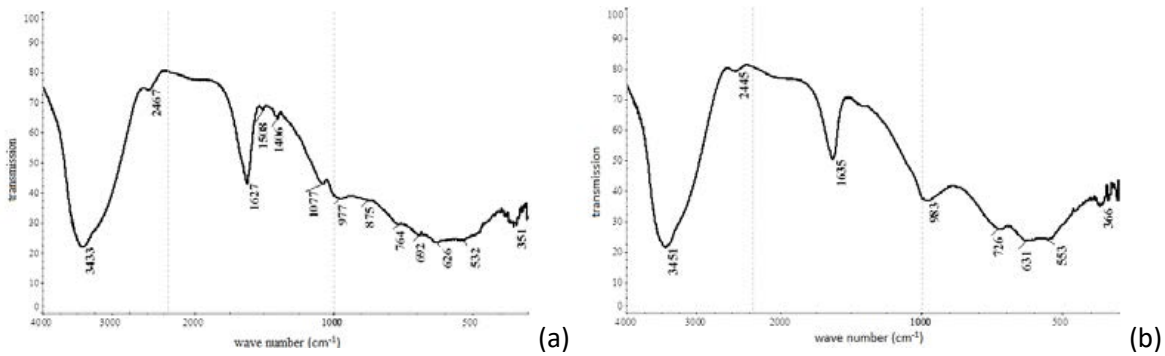

Fig. 9: IR spectra of Coagulants No. 11 (a) and No. 15 (b) as tablets with KBr

(2013) and Tang *et al*. (2015), increasing charges were strong enough to impede further cluster access. The efficiency of the aluminum oxychloride coagulant $Al_x(OH)_yCl_{3x-y}\cdot zH_2O$ depended on its basicity. The high efficiency of aluminum oxychloride was probably due to the establishment of equilibrium between cations in the adsorption layer of colloidal particles and hydrolysis in the solution of excess coagulants. Hydrophobic colloids of low soluble aluminum hydroxides or their basic salts were formed as results of hydrolysis, depending on the pH of the medium. These colloids had huge active surfaces and play major roles. This assumption is consistent with the existing opinions of authors (Grechanikov *et al*., 2010; Zhao *et al*., 2015). The colloidal particles of impurities were adsorbed on the surfaces of colloidal hydroxide particles coagulated under the actions of electrolytes dissolved in water to form flakes, which sorbed and captured the impurities in the water during settling. As a result of these processes, the aggregative stability of the system was disturbed resulting in the formation of macrodispersion separated through sedimentation, flotation, and filtration (Wei *et al*., 2015). As noted above, the obtained reagents were tested in the treatment of different types of natural drinking water ("Almaty Su" and "Medeu" water intakes), recycled water from water treatment units, including oil-contaminated wastewater (Sample Nos. 1 and 2) from various enterprises of Kazakhstan. Coagulants Nos. 11, 15, and 20 were tested as RAS samples. The main characteristics of coagulants are shown in Table 5.

Water quality control, from the "Almaty Su" water intake before and after treatment, was performed for the main parameters of water quality: pH International Organization for Standardization (ISO) 110523-2008, turbidity ISO 7027-1-2016, permanganate acidity; chemical oxygen demand (COD), ISO 6060-1989, salt content, oil ISO 9377-2. Tables 7 and 8 show the comparative results of water turbidity measurements after treatment with coagulants. Based on the data in Table 6, turbidity decreased from 16.8 to 0.47 Formazin Nephelometric Unit (FNU), the effectiveness of turbidity reduction reached 97.2%, and water quality improved as pH of water increased to 9–9.5. Coagulant No. 20 based on activated Rau-97 alloy was effective for the treatment of oil-contaminated wastewater (Table 7). Water turbidity was 44.4 FNU before treatment. It was 0.37 FNU after the treatment with the coagulant in the dosage of 5 milliliter per cubic decimeter (mL/dm^3)of 0.1% of Al_2O_3 solution (pH 4.35). Purification efficiency reached 99.16%.

Water from the "Almaty SU" water intake after treatment with Coagulant No. 15 at a dose of 10 mg/L had permanganate oxidation equal to −2.2 milligram of Oxygen per liter ($mg0_2$/L). The comparative results of the permanganate acidity of water depending on pH after treatment with Coagulant No. 15 enabled to conclude that the permanganate acidity of water samples increased from 1.17 $mg0_2$/L to 2.70 $mg0_2$/L with pH increase from 5.0 to 7.5. An increase in pH up to 9 with a coagulant treatment reduced permanganate oxidation to 1.87 $mg0_2$/L, which is within normal limits. The average permanganate acidity for drinking water was 2.6 $mg0_2$/L. The results of turbidity measurement, treatment efficiency assessment for natural and oil-contaminated

wastewater (Sample no. 1), and circulating water of a water treatment unit after treatment with 0.1% Al_2O_3 solution of Coagulant No. 20 based on aluminum alloy Rau-97 are shown in Table 7 and Fig. 10.

Based on the data of water analysis using the industively coupled plasma method, the contents

Table 5: Main characteristics of and conditions for obtaining aluminum polyoxychloride solutions based on AAAs

Coagulant cipher	Terms of test				Main characteristics of coagulants			
	Alloy	Reaction temperature, ℃	HCl content, % by mass in solution	Amount of added HCl, mL	Mass fraction of Al converted to Al_2O_3, in ,(dry)%	Basicity, %	Electrical conductivity, mS/cm	pH
No. 11	Rau-85	25	3.0	50	31.0	66.9	30.5	3.29
No. 15	Rau-97	90	1.0	50	33.1	62.70	22.8	3.52
No. 20	Rau-97	25	3.0	50	33.0	56.20	27.8	3.28

Alloy weight: 1 g

Table 6: Comparative results of turbidity measurement and assessment of effectiveness of natural water treatment from "Almaty SU" water intake with 10% Coagulant solution No. 15 at different pH of water (coagulant dose 10 mg/L)

pH of Source water	Water pH after treatment	Water turbidity after treatment, FNU	Removal efficiency (%)
5.0	5.7	7.51	55.30
6.5	6.7	0.63	96.25
7.5	6.9	0.83	95.06
9.0	8.4	0.47	97.20
9.5	8.9	0.60	96.43

Almaty SU water (07.07.2022) (before treatment) pH: 6.5–6.8, turbidity (16.8) FNU (9.74 mg/L kaolin). According to the standards of SanPiN 2.1.4.1074-01, the turbidity of drinking water must not exceed 2.6 FNU or 1.5 mg/L kaolin (FNU 0.58)

Table 7: Results of turbidity measurement and efficiency assessment for natural water and wastewater treatment with 0.1% solution in terms of Al_2O_3 of coagulant No. 20 based on aluminum alloy Rau-97

Water sample, turbidity	Coagulant dose, mL/dm^3	Water pH		Turbidity, FNU	Removal efficiency (%)
		Before treatment	After treatment		
Natural "Almaty Su" 4.52 FNU	0.1	7.34	7.43	0.48	89.38
	0.5	7.38	7.48	0.32	92.92
	1.0	7.25	7.23	0.53	88.27
	5.0	7.25	7.13	0.62	86.28
	10	7.25	7.01	0.64	85.84
Natural Medeu 26.1 FNU.	0.02	7.12	7.15	1.98	92.41
	0.10	7.15	7.28	1.20	95.40
	1.0	7.15	7.28	0.82	96.86
	5.0	7.12	7.05	0.67	97.43
Oil-contaminated wastewater (Sample No. 1) 44.4 FNU	1.0	7.04	7.44	6.19	86.06
	1.5	7.38	7.17	0.99	97.77*
	1.5	7.38	7.24	0.69	98.45
	2.0	7.38	7.17	0.55	98.76
	3.0	7.37	7.30	0.62	98.60
	4.0	7.37	7.25	0.42	99.05
	5.0	7.04	7.54	0.37	99.17

*Coagulant PAC Aqua-Aurat-30

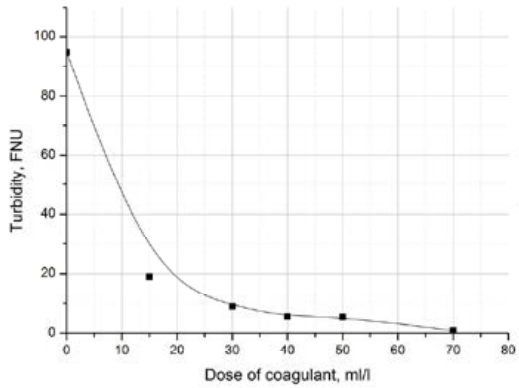

Fig. 10: Change in the turbidity of recycled water from a water treatment unit treated with 0.1% solution per Al_2O_3 of Coagulant No. 20

Table 8: Oil content in wastewater (Sample no. 1) treated with 0.1% solution in terms of Al_2O_3 of coagulant PAC No. 20.

Dose of PAC (mL/dm^3)	pH before treatment	pH after treatment	Oil content (mg/L)	Removal efficiency (%)
1.0	7.04	7.44	1.02	34.62
1.5	7.38	7.24	0.78	50.00
2.0	7.38	7.17	0.56	64.10
3.0	7.37	7.30	0.60	61.54
4.0	7.37	7.25	0.60	61.54
5.0	7.04	7.54	0.42	73.08

Oil content in water sample was 1.56 mg/L.

of Fe, calcium (Ca), and magnesium (Mg) cations significantly decreased after water sample treatment. Thus, the content of Fe cations decreased from 3.85 g/L to 0.049 g/L, Ca from 0.727 g/L to 0.713 g/L, Mg from 0.235 g/L to 0.202 g/L for oil-polluted wastewater after treatment with Coagulant No. 20 (1.5 mL/dm^3 of 0.1% solution in terms of Al_2O_3) (Sample No. 1). The oil content in wastewater (Sample no. 1) treated with 0.1% solution in terms of Al_2O_3 of Coagulant PAC No. 20 decreased from 1.56 mg/L to 0.42 mg/L (Table 8). Purification efficiency was 73.1%.

The permanganate oxidation of oily contaminated wastewater (Sample no. 1) with 0.1% solution in recalculation on Al_2O_3 of Coagulant No. 20 decreased from 50.05 mg O_2/L to 45.27 mg O_2/L. The assessment of oil-contaminated water treatment efficiency was also performed for oil-contaminated wastewater (Sample no. 2). Water characteristics before treatment with aluminum polyoxychloride are specified in Table 9.

Oil content was determined with spectrophotometer SPEKOL 1300 (Analytik Jena), extraction with chloroform. The wastewater treatment (Sample No. 2) with a coagulant in an amount of 10–20 µl/L resulted in the decrease of oil content from 8.85 mg/L to 0.86 mg/L. The efficiency of cleaning with Coagulant No. 11 was 90.28 %. The particle size of oil and zeta potential of oil-contaminated wastewater (Sample no. 2) was studied before and after the coagulant treatment using particle size analyzer Malvern Zetasizer NanoZS 90. The device enabled to measure particles from 0.3 nm to 10 microns (dynamic light scattering method) using noninvasive backscattering technology. The minimum sample amount was 20 µL. The accuracy was ± 2%. The M3-PALS method of electrophoretic light scattering was used to measure zeta potential in aqueous and anhydrous disperse systems. In this regard, the manufacturers of the device recommend using water with a particle size of 3.8 nm–100 µm for analysis. Six samples of oil-contaminated wastewater (Sample No. 2) with oil content of 8.85 mg/L) with different dosage of coagulants were prepared for measurements in the present work. Each sample was analyzed 12 times for particle size determination and 3 times for zeta potential determination with the average value derived. The working temperature

of the measurement was 25 °C. The refractive index was 1.4, and the absorption coefficient was 1 for oil according to the reference data. In Grechanikov *et al.*, (2010), the zeta potential is usually from −14 to −30 mV for colloids present in water having pH = 5–8. The greater its negative value, the greater the magnitude of the particle charge. Elkhova *et al*. (2006) revealed that when the zeta potential decreases, the distance between particles decreases, which increases the probabilities of their collisions. Coagulants create positive charges in water treatment systems with pH = 6–8, which decrease the zeta potential value. The authors point out that coagulation usually proceeds with a small negative zeta potential value, so that the complete neutralization of the charge is not required. However, when the coagulant is overdosed, the surface of a particle becomes positively charged, and the particles reenters the dispersed phase. The main results of the determination of oil particle sizes and zeta potentials of wastewater before and after treatment with coagulants in comparison with the Rau-85 reagent are shown in Table 10. The zeta potential of wastewater was negative –28.6 mV, the oil particle radius in the initial wastewater was 19.09 nm, the average particle radius was 90.44 nm, and the polydispersity index was 0.245. The oil particle radius in the wastewater reached 60.18 nm after wastewater treatment with the Rau-85 reagent in an amount of 10 m/L. The average radius was 100.2 nm, the polydispersity index was 0.325, and the average value of zeta potential was –28.4 mV.

After wastewater treatment with the Rau-85 reagent of 100 mg/dm^3, the particle radius increased to 647.4 nm, the average radius was 764.2 nm, the polydispersity index was 0.244, and the average value of zeta potential was −22.3 mV. The average particle radius increased up to 7901 nm, the polydispersity index was 0.101, and the average value of zeta potential reached −18.8 mV in wastewater after treatment with Coagulant No. 11. The data obtained allowed to conclude that oil particle size increased and a change occurred in the zeta potential toward zero with an increase in the dose of reagents, indicating that the system became less stable and was prone to coagulation and precipitation. Note that the most accurate particle size results can be obtained when the polydispersity index is less than 0.1, i.e., for spherical particles. The average particle size (radius) can be used for comparative purposes for slightly large polydispersity values. Relying on the average value is inappropriate, and the distribution analysis should be used to determine peak positions for broad distributions where the polydispersity is greater than 0.5.

Table 9: Physical and chemical properties of oil-contaminated wastewater (Sample no. 2)

Water sample	Density, kg/cm^3	pH	Electrical conductivity, mS/cm	Total salt content, mg/L	Oil content, mg/L
Oil-contaminated wastewater (Sample No. 2)	998	6.91	311	174.0	8.85

Table 10: Comparative results of oil particle size and zeta potential of oil-contaminated wastewater (Sample No. 2) before and after treatment with coagulants

Sample	Particle radius (nm)	Average particle radius (nm)	Polydispersity index	Zeta potential (mV)
Wastewater (Sample No. 2)	19.09	90.44	0.245	−28.6
Wastewater (Sample no. 2) treated with 10 mg/dm^3 Rau-85	60.18	100.2	0.325	−28.4
Wastewater (Sample No. 2) treated with 100 mg/dm^3 Rau-85	647.4	764.2	0.244	−22.3
Wastewater (Sample No. 2) treated with 10 µl/L of Coagulant No. 11	21.69	90.14	0.264	−29.1
Wastewater (Sample No. 2) treated with 100 µl/L of Coagulant No. 11	No peaks in the measured range	7901	0.101	−18.9
Wastewater, (Sample no. 2) treated with 100 µl/L of Coagulant No. 8	No peaks in the measured range	$2.775 \cdot 10^4$	1.0	−14.2

Particle Size Analyzer Malvern Zetasizer Nano ZS 90;
Coagulant No. 8 based on Rau-85, basicity 22.38%, mass fraction of Al_2O_3 −15.75% (solution), pH 2.24

CONCLUSIONS

A principally new approach to the development of a technology intended to obtain aluminum polyoxychloride coagulants for water treatment from natural and anthropogenic polution sources was theoretically substantiated and experimentally proven. The regularities of obtaining basic aluminum chloride (PAC) on the basis of AAAs containing metal activators—Ga, In, and Sn with contents from 0.5 wt% to 5 wt% (Rau-98.5, Rau-97, and Rau-85)—were studied. A method intended to produce aluminum polyoxychloride used as a coagulant for a potable water treatment was developed, considering existing disadvantages of known methods. The method involved treatment with 1%–5% HCl for 2–3 hours of AAAs containing metals in the following ratio (wt%): In 0.5–5, Ga 0.5–5, Sn 0.5–5, and aluminum is the rest. The developed method provided aluminum polyoxychloride with the necessary degree of basicity 41%–82.6% and with a mass fraction of aluminum in terms of Al_2O_3 of 30%–48%. The process was performed under mild conditions at an initial temperature of 20 °C–25 °C. Then, the temperature rose up to 60 °C–65 °C maintained at the expense of the exothermic dissolution reaction heat of activated aluminum-containing alloys in HCl. The microstructure, phase component, elemental composition of aluminum polyoxychloride were studied with the use of a sufficient number of analytical and instrumental methods—IR spectroscopy, XRD, SEM with EDS, XRF, and X-ray spectral analysis. The effectiveness of the purification of water samples taken from "Almaty Su" and "Medeu" water intake stations, recycled water of a cooling water treatment unit, and oil-contaminated wastewater (anthropogenic pollution sources) was assessed. Treated water parameters were within the standards established for drinking water supply and wastewater disposal intended for water discharge into the receiving facility. The reduction of the turbidity of water sampled from the "Almaty Su" water intake station reached 97.2% and that of recycled water reached −99.6%. The efficiency of the treatment of oil-contaminated wastewater from oil reached 90.27%. This research intended to determine oil particle size and the zeta potential of oil-contaminated wastewater. It concluded that oil particle size increased and the zeta potential of water toward zero changes with an increase in coagulant dosage, indicating that the system becomes less stable, prone to coagulation and precipitation. The results confirm that aluminum polyoxychloride is an effective coagulant for potable and wastewater treatment. The treated water is within the established limits for hydrogen potential, COD, and turbidity. The water treatment method can be easily implemented.

AUTHOR CONTRIBUTIONS

R.G. Sarmurzina defined the concept, selected and justified the research direction. G.I. Boiko determined the purposes and objectives of the study, supervised the research, verified and edited the manuscript. B.K. Kenzhaliyev attracted funding and perfomed the research methodologies. N.P. Lyubchenko analyzed and interpreted the data and prepared the manuscript text. P.V. Kenyaikin performed the experiments, figures, tables, and graphical abstracts. U.S. Karabalin perfomed consultation and analyzed the research results. Zh.B. Ilmaliev analysed the results of instrumental methods of the study.

ACKNOWLEDGMENT

The experiment was conducted in Satbayev University, AO "Institute of Metallurgy and Ore Beneficiation" Republic of Kazakhstan, Almaty, 050010 Shevchenko 29/133, E-mail: imio@imio.kz. The work was performed at the expense of the program-targeted funding of the Ministry of Science and Higher Education of the Republic of Kazakhstan [IRN BR11765599].

CONFLICT OF INTEREST

The author declares no conflict of interest regarding the publication of this manuscript. Ethical issues, including plagiarism, informed consent, misconduct, data fabrication and/or falsification, double publication and/or submission, and redundancy, have been completely observed by the authors.

OPEN ACCESS

ABBREVIATIONS

%	Percent
°C	Degrees Celsius
µm	Micrometers
^{0}C/min	Degrees Celsius per minute
A.C.S.	American Chemical Society
AAA	Activated aluminum alloys
AC	Aluminum chloride
Al	Aluminium
Al_2O_3	Aluminium oxide
BCC	Body-centered cubic structure
Bi	Bismuth
Ca	Calcium
Cd	Cadmium
Cl	Chlorine
Cu	Copper
DTA	Differential thermal analysis
DTG	Derivative thermogravimetric
EDX	Energy dispersive X-rays
EDXS	Energy-dispersive X-ray spectroscopy
ERG	Eurasian Group
FCC	Face-centered cubic
Fe	Iron
FNU	Formazine Nephelometric Unit – formazine turbidity unit
FTIR	Fourier-transform infrared
g	Grams
g/cm³	Grams per cubic centimeter
Ga	Gallium
GB	GuoBiao
HCl	Hydrochloric acid
OH	Hydroxyl
In	Indium
IR Spectrum	Infared spectrum
ISO	International organization for standardization
JSC	Joint-stock company
K	Kelvin
KBr	Potassium bromate
kg	Kilogram
kg/cm³	Kilogram per centimeter in a cube
kV	Kilovolt
Ltd	Limited trade development
mA	Milliamp
Mg	Magnesium
mg/L	Milligram per liter
mgO_2/L	Milligram of oxygen per liter
min	Minut
mL	Millilite
mL /min	Milliliters per minute
mL/dm³	Milliliter per cubic decimeter
mL/g min	Milliliter per gram per minute
mm	Millimeter
mV	Millivolt
nA	Nanoamper
NIBS	Non-invasive backscatter
nm	Nanometer
NTU	Nephelometric turbidity units
Pb	Lead
PDF	Powder diffractometer database
pH	Hydrogen potential
PAC	Poly aluminium chloride
rpm	Revolutions per minute
Sn	Tin
STA	Simultaneous thermal analyzer
SEM	Scanning electron microscope
TG	Thermogram
wt	Weight
XRD	X-ray diffraction analysis
XRF	X-ray phase analysis
Zn	Zinc

REFERENCES

Chen, S.; Yuan, Z.; Hanigan, D.; Westerhoff, P.; Zhao, H.; Ni, J., (2018). Coagulation behaviors of new covalently bound hybrid coagulants (cbhyc) in surface water treatment. Sep. Purif. Technol., 192: 322-328 **(7 pages).**

Dayarathne, H.N.P.; Angove, M.J.; Aryal, R.; Abuel-Naga, H.; Mainali, B., (2021). Removal of natural organic matter from source water: review on coagulants, dual coagulation, alternative coagulants, and mechanisms. J. Water Process Eng., 40: 101820 **(13 pages).**

Du, B.D.; He, T.T.; Liu, G.L.; Chen, W.; Wang, Y.M.; Wang, W.; Chen, D.M., (2018). Al-water reactivity of al-mg-ga-in-sn alloys used for hydraulic fracturing tools. Int. J. Hydrogen Energy. 43(15): 7201-7215 **(15 pages).**

Elkhova, V.D.; Abdrakhimov, Y.R.; Elkhov, A.A.; Luchinina, A.A.; Tikhonova, E.A., (2006). Production of new high-performance coagulants from production waste. Bashkir Chem. J., 13(3): 31-35 **(5 pages).**

Grechanikov, A.V.; Platonov, A.P.; Trutnev, A.A.; Kovchur, C.G., Гречаников A.B., (2010). Water-soluble polyelectrolytes - flocculants in water treatment processes. Vestnik Vitebsk Stat. Tech. Univ., 2(19): 107-111 **(5 pages).**

He, T.; Chen, W.; Wang, W.; Ren, F.; Stock, H.-R., (2020a). Effect of different cu contents on the microstructure and hydrogen production of al-cu-ga-in-sn alloys for dissolvable materials. J. Alloys Compd., 821(2020): 153489 **(7 pages).**

He, T.; Chen, W.; Wang, W.; Du, S.; Deng, S., (2020b). Microstructure and hydrogen production of the rapidly solidified al-mg-ga-in-sn alloy. J. Alloys Compd., 827(2020): 154290 **(7 pages).**

He, T.; Wang, W.; Chen, W.; Chen, D.; Yang, K., (2017a). Reactivity of al-rich alloys with water promoted by liquid Al grain boundary phases. J. Mater. Sci. Technol., 33(4): 397-403 **(7 pages).**

He, T.T.; Wang, W.; Chen, W.; Chen, D.M.; Yang, K., (2017b). Influence of in and sn compositions on the reactivity of al-ga-in-sn alloys with water. Int. J. Hydrogen Energy, 42(9): 5627-5637 **(11 pages).**

He, W.; Xie, Z.; Lua, W.; Huang, M.; Ma, J., (2019). Comparative analysis on floc growth behaviors during ballasted flocculation by using aluminum sulphate (as) and polyaluminum chloride (pacl) as coagulants. Sep. Purif. Technol., 213(2019): 176-185 **(10 pages).**

Jiao, R.; Xu, H.; Xu, W.; Yang, X.; Wang, D., (2015). Influence of coagulation mechanisms on the residual aluminum – the roles of coagulant species and mw of organic matter. J. Hazard. Mater., 290(2015): 16-25 **(10 pages).**

Kumar, D.; Muthukumar, K., (2020). An overview on activation of aluminium-water reaction for enhanced hydrogen production. J. Alloys Compd., 835(2020): 155189 **(10 pages).**

Lee, C.H.; Tiwari, B.; Zhanga, D.; Yap, Y.K., (2017). Water purification: oil–water separation by nanotechnology and environmental concerns. Environ. Sci.: Nano, 4(2017): 514-525 **(12 pages).**

Li, F.; Jiang, J.-Q.; Wu, S.; Zhang, B., (2010). Preparation and performance of a high purity poly-aluminum chloride. Chem. Eng. J. 156: 64–69 **(6 pages).**

Lyakishev, N.P., (1996). State diagrams of binary metal systems, 1st. V. Mashinostroyeniye.

Masakbaeva, S.R.; Tokareva, A.V.; Nesmeyanova, R.M.; Kovtareva, S.Y., (2021). Preparation of aluminum oxychloride from aluminum hydroxide and hydrochloric acid. Sci.Technol. Kazakhstan, 1: 6-11 **(6 pages).**

Nakamoto, K., (2009). Infrared and raman spectra of inorganic and coordination compounds, 6th. Ed. John Wiley and Sons Inc.

Novakov, I.A.; Radchenko, P.S., (2013). Alumoxane nanoparticles as the precurcors for the novel organic-inorganic hybrid polymer compositions. Izvestia Volgograd Technical University. 10(4): 5-20 **(16 pages)**.

Pini, M.; Breglia, G.; Venturelli, M.; Montorsi, L.; Milani, M.; Neri, P.; Ferrari A.M., (2020). Life cycle assessment of an innovative cogeneration system based on the aluminum combustion with water. Renewable Energy. 154(2020): 532-541 **(10 pages).**

Qiao, D.; Lu, Y.; Tang, Z.; Fan, X.; Wang, T.; Li, T.; Liaw, P.K., (2019). The superior hydrogen-generation performance of multi-component al alloys by the hydrolysis reaction. Int. J. Hydrogen Energy, 44(7): 3527-3537 **(11 pages).**

Sarmurzina, R.G.; Boiko, G.I.; Lyubchenko, N.P.; Karabalin, U.S.; Demeubayeva, N.S., (2022a). Alloys for the production of hydrogen and active aluminum oxide. News Natl. Acad. Sci. R.K. Ser. Geol. Tech. Sci., 1(451): 91-98 **(8 pages).**

Sarmurzina, R.G.; Boiko, G.I.; Lyubchenko, N.P.; Karabalin, U.S.; Yeligbayeva, G.Z. Demeubayeva, N.S., (2022b). Hydrogen obtaining from the system activated aluminum – water. News Natl. Acad. Sci. R. K. Ser. Geol. Tech. Sci., 6(456): 196-213 **(17 pages).**

Sarmurzina, R.G.; Boiko, G.I.; Baigaziyev M.T.; Karabalin, U.S.; Lyubchenko, N.P., (2018). New generation of energy accumulating substances on the basis of activated aluminum. J. Chem. Technol. Metall., 53(1): 119-124 **(6 pages).**

Shamaei, L.; Khorshidia, B.; Perdicakis, B.; Sadrzadeh, M., (2018). Treatment of oil sands produced water using combined electrocoagulation and chemical coagulation techniques. Sci. Total Environ., 645(2018): 560-572 **(13 pages).**

Sun, H.; Jiao, R.; Xu, H.; An, G.; Wang, D., (2019). Effect of particle size and concentration in combination with ph on coagulation mechanisms. J. Environ. Sci., 82: 39-46 **(8 pages).**

Sychev, A.V.; Sychev, S.A.; Rashkovsky, G.B., (2015). Method of producing aluminium oxychloride, Rus. Patent 2589164C1.

Tang, H.; Xiao, F.; Wang, D., (2015). Speciation, stability, and coagulation mechanisms of hydroxyl aluminum clusters formed by pacl and alum: a critical review. Adv. Colloid Interface Sci., 226(A): 78-85 **(8 pages).**

Tokareva, A.V.; Masakbaeva, S.R., (2020). Aluminum oxychloride coagulant for drinking water treatment. Sci. Technol. Kazakhstan, 2(2020): 58–65 **(8 pages).**

Trowell, K.A., Goroshin, S.; Frost, D.L.; Bergthorson, J.M., (2020) Aluminum and its role as a recyclable, sustainable carrier of renewable energy. Appl. Energy. 275: 115112 **(8 pages)**.

Wang, W.; Zhao, x.M.; Chen, D.M.; Yang, K., (2012). Insight into the reactivity of al-ga-in-sn alloy with water. Int. J. Hydrogen Energy. 37(3): 2187-2194 **(8 pages).**

Wang, X.; Gan, Y.; Guo, S.; Ma, X.; Xu, M.; Zhang, S., (2018). Advantages of titanium xerogel over titanium tetrachloride and polytitanium tetrachloride in coagulation: a mechanism analysis. Water Res., 132: 350-360 **(11 Pages).**

Wei, C.; Liu, D.; Xu, S.; Cui, T.; An, Q.; Liu, Z.; Gao, Q., (2018). Effects of cu additives on the hydrogen generation performance of al-rich alloys. J. Alloys Compd., 738: 105-110 **(6 pages).**

Wei, N.; Zhang, Z.; Liu, D.; Wu, Y.; Wang, J.; Wang, Q., (2015). Coagulation behavior of polyaluminum chloride: effects of ph and coagulant dosage. Chin. J. Chem. Eng., 23(6): 1041–1046 **(6 pages).**

Xiao, F.; Guo, Y.; Yang, R.; Li, J., (2019). Hydrogen generation from hydrolysis of activated magnesium/low-melting-point metals alloys. Int. J. Hydrogen Energy, 44(3): 1366-1373 **(8 pages).**

Xiao, F.; Ma, J.; Yi, P.; Huang, J.-C.H., (2008). Effects of low temperature on coagulation of kaolinite suspensions. Water Res., 42 (12): 2983-2992 **(10 pages).**

Yang, B.; Zhu, J.; Jiang, T.; Gou, Y.; Hou,X.; Pan, B., (2017). Effect of heat treatment on Al-mg-ga-in-sn alloy for hydrogen generation through hydrolysis reaction. Int. J. Hydrogen Energy. 42(38): 24393-24403 **(11 pages)**.

Zhang, Z.; Wang, J.; Liu, D.; Li, J.; Wang, X.; Song, B.; Yue, B.; Zhao, K.; Song, Y., (2017). Hydrolysis of polyaluminum chloride prior to coagulation: effects on coagulation behavior and implications for improving

coagulation performance. J. Environ. Sci., 57: 162–169 **(8 pages)**.
Zhao, Y.X.; Phuntsho, S.; Gao, B.Y.; Yang, Y.Z.; Kim, J.H.; Shon, H.K., (2015). Comparison of a novel polytitanium chloride coagulant with polyaluminium chloride: coagulation per-formance and floc characteristics. J. Environ. Manage., 147: 194–202 **(9 pages).**
Zhao, Y.X.; Gao, B.Y.; Shon, H.K.; Cao, B.C.; Kim, J.-H., (2011). Coagulation characteristics of titanium (ti) salt coagulant compared with aluminum (al) and iron (fe) salts. J. Hazard. Mater., 185: 1536-1542 **(7 pages).**

AUTHOR (S) BIOSKETCHES

Sarmurzina, R.G., Ph.D., Professor, Academician of KazNAEN, Honorary Academician of NAS RK Association of Producers and Consumers of Petrochemical Products, Satbayev University, Institute of Metallurgy and Ore Beneficiation JSC, Almaty, Kazakhstan.
- Email: *sarmurzina_r@mail.ru*
- ORCID: 0000-0002-9572-9712
- Web of Science ResearcherID: HNI-8501-2023
- Scopus Author ID: 6603381995
- Homepage: https://official.satbayev.university/en/vnedrennye-proekty/ap09260008-aktivirovannyy-alyuminiy-kak-alternativnyy-istochnik-energii-i-vodoroda-v-reshenii-slozhnykh-ekologicheskikh-problem-neftyanoy-otrasli

Boiko, G.I., Ph.D., Professor, Satbayev University, Institute of Metallurgy and Ore Beneficiation JSC, Almaty, Kazakhstan.
- Email: *galina.boyko.kaznitu@gmail.com*
- ORCID: 0000-0002-2912-3384
- Web of Science ResearcherID: AAF-4591-2019
- Scopus Author ID: 7006693195
- Homepage: https://official.satbayev.university/en/teachers/galina-i-boyko-

Kenzhaliyev, B.K., Ph.D., Professor, Director Institute of Metallurgy and Enrichment, Satbayev University, Institute of Metallurgy and Ore Beneficiation JSC, Almaty, Kazakhstan.
- Email: *bagdaulet_k@mail.ru*
- ORCID: 0000-0003-1474-8354
- Web of Science ResearcherID: N-9602-2017
- Scopus Author ID: 6603486541
- Homepage: https://imio.kz/en/our-researchers/

Karabalin, U.S., Ph.D., Professor, Academician of the National Engineering Academy of the Republic of Kazakhstan, Academician of the International Engineering Academy, Honorary Professor of the Kazakh National Technical University «Kazenergy» Association, KAZENERGY Association, Astana, Kazakhstan.
- Email: *reception@kazenergy.com*
- ORCID: 0000-0002-7471-7851
- Scopus Author ID: 56105006900
- Homepage: https://www.kazenergy.com/en/association/structure/853/

Lyubchenko, N.P., Ph.D. Candidate of chemical sciences, Satbayev University, Institute of Metallurgy and Ore Beneficiation JSC, Almaty, Kazakhstan.
- Email: *amtek@bk.ru*
- ORCID: 0000-0002-7133-808X
- Web of Science ResearcherID: HNI-7755-2023
- Scopus Author ID: 6507764144
- Homepage: https://official.satbayev.university/en/vnedrennye-proekty/ap09260008-aktivirovannyy-alyuminiy-kak-alternativnyy-istochnik-energii-i-vodoroda-v-reshenii-slozhnykh-ekologicheskikh-problem-neftyanoy-otrasli

Kenyaikin, P.V., M.Sc., Satbayev University, Institute of Metallurgy and Ore Beneficiation JSC, Almaty, Kazakhstan.
- Email: *kenyaikin.p@gmail.com*
- ORCID: 0000-0002-4360-1573
- Web of Science ResearcherID: ABY-5675-2022
- Scopus Author ID: NA
- Homepage: https://official.satbayev.university/en/vnedrennye-proekty/ap09260008-aktivirovannyy-alyuminiy-kak-alternativnyy-istochnik-energii-i-vodoroda-v-reshenii-slozhnykh-ekologicheskikh-problem-neftyanoy-otrasli

Ilmaliyev, Zh.B., Ph.D. *Candidate* of *Legal Sciences*, Satbayev University, Institute of Metallurgy and Ore Beneficiation JSC, Almaty, Kazakhstan.
- Email: *jans2009@mail.ru*
- ORCID: 0000-0002-7133-808X
- Web of Science ResearcherID: N-7444-2017
- Scopus Author ID: 57205448266
- Homepage: https://imio.kz/en/our-researchers/

HOW TO CITE THIS ARTICLE

Sarmurzina, R.G., Boiko, G.I., Kenzhaliyev, B.K., Karabalin, U.S., Lyubchenko, N.P., Kenyaikin, P.V., Ilmaliyev, Zh.B., (2023). Coagulants for water based on activated aluminum alloys. Global J. Environ. Sci. Manage., 9(4): 673-690.

DOI: 10.22035/gjesm.2023.04.02

URL: https://www.gjesm.net/article_703090.html